Atmospheric Research 224 (2019) 42–51

Contents lists available at ScienceDirect

Atmospheric Research

journal homepage: www.elsevier.com/locate/atmosres

Adverse results of the economic crisis: A study on the emergence of enhanced formaldehyde (HCHO) levels seen from satellites over Greek urban sites

I. Zyrichidou[a,*], D. Balis[a], M.E. Koukouli[a], T. Drosoglou[a], A. Bais[a], M. Gratsea[b,c], E. Gerasopoulos[b], N. Liora[a], A. Poupkou[a], C. Giannaros[a], D. Melas[a], I. De Smedt[d], M. Van Roozendael[d], R.J. Van der A[e], K.F. Boersma[e,f], P. Valks[g], A. Richter[h]

[a] Laboratory of Atmospheric Physics, Physics Department, AU. Th, Thessaloniki, Greece
[b] Institute for Environmental Research and Sustainable Development, National Observatory of Athens, Greece
[c] Environmental Chemical Processes Laboratory, Department of Chemistry, University of Crete, Greece
[d] Royal Belgian Institute for Space Aeronomy (BIRA-IASB), Brussels, Belgium
[e] Royal Netherlands Meteorological Institute (KNMI), De Bilt, The Netherlands
[f] Wageningen University, Meteorology and Air Quality Group, Wageningen, The Netherlands
[g] DLR-IMF, Wessling, Germany
[h] Institute of Environmental Physics and Remote Sensing, University of Bremen (IUP-UB), Bremen, Germany

ARTICLE INFO

Keywords:
HCHO
GOME-2 instrument
Urban air pollution
NO_2
Biomass burning

ABSTRACT

In order to study the years of the outbreak of the financial crisis in Greece, we use a continuous eight-year record (2008–2015) of formaldehyde, HCHO, columns retrieved from the GOME-2/MetOp-A and GOME-2/MetOp-B satellite instruments over two urban Greek regions, Thessaloniki and Athens. A statistical linear regression analysis that was applied to the GOME-2/MetOp-A HCHO time series over both cities revealed positive annual changes. On seasonal basis, the wintertime HCHO change per annum was found to be 7.43 ± 2.26% and 6.13 ± 2.12% over Thessaloniki and Athens, respectively. A corresponding seasonal time series analysis was also applied to tropospheric nitrogen dioxide, NO_2, levels. The tropospheric NO_2 winter change per annum is shown to be negative, at −3.0 ± 0.13% and −3.94 ± 0.14% over Thessaloniki and Athens, respectively. The satellite HCHO and NO_2 observations levels are comparable to collocated ground-based MAX-DOAS measurements. Furthermore, the Comprehensive Air Quality Model with extensions chemical transport model, CAMx CTM, as well as the driving emission inventory in CAMx are used for further investigation of the seasonality of the HCHO concentrations and emissions. The CTM model analysis of the annual HCHO cycle and the winter season anti-correlation between HCHO total columns and surface temperature, mostly over Thessaloniki (R = –0.3), point to the fact that the winter HCHO enhancements, likely connected with enhanced anthropogenic activities, are not being captured by the model. The results of this study indicate a possible enhanced anthropogenic activity during the winter season that was strengthened through the investigation on the origins of the wintertime increase in HCHO columns since the beginning of the economic crisis in the country.

1. Introduction

Formaldehyde (HCHO) is a principal intermediate in the basic oxidation cycles of hydrocarbons and a number of radicals. Oxidation of methane (CH_4) by the hydroxyl radical (OH) is the major principal source of HCHO in most of the troposphere (e.g. Lowe and Schmidt, 1983; Singh et al., 2000). In the continental boundary layer, it is locally emitted by the oxidation of Non-Methane Volatile Organic Compounds (NMVOCs) (mostly isoprene) (Fried et al., 2003). It is also produced directly by vegetation (Lathiere et al., 2006; Seco et al., 2007) and as a secondary product during biomass burning cases (e.g. Lee et al., 1997; Andreae and Merlet, 2001). Loss of HCHO is mainly by photolysis ($HCHO \rightarrow CO + H_2$ or $HCO + H$) at wavelengths below 400 nm, reaction with atmospheric OH ($HCHO + OH \rightarrow HCO + H_2O$) as well as wet and dry deposition. This results in a lifetime that is short enough, of the order of some hours during midday (e.g. Sander et al., 2006), not to be

* Corresponding author.
E-mail address: ezyrichi@auth.gr (I. Zyrichidou).

https://doi.org/10.1016/j.atmosres.2019.03.017
Received 14 May 2018; Received in revised form 12 March 2019; Accepted 17 March 2019
Available online 18 March 2019
0169-8095/

significantly affected by transport (Shim et al., 2005). This lifetime decreases with increasing altitude due to an enhanced photolysis rate. As a consequence of its rather short lifetime, elevated HCHO levels are typically found next to their primary sources (e.g. Marbach et al., 2009; Stavrakou et al., 2009). Although the biogenic sources are dominant in the background troposphere, at least during the vegetative season, the anthropogenic origin of VOCs is also important in densely populated environments. Direct (primary) emissions by anthropogenic sources is the main source in populated and industrialized areas, such as via industrial processes, incomplete combustion of biomass and fossil fuel, motor vehicles (as in Anderson et al., 1996; Lawson et al., 1990). According to Stavrakou et al. (2009), although the contribution of directly released HCHO is minor (< 1%) on the global total, it can be significant on local scale, particularly during fire events.

A change in the anthropogenic activities is undoubtedly associated with a change in the emissions of air pollutants affecting human health (Favez et al., 2010). Several previous studies have recently looked into and suggested the connection between the onset of the economic crisis and the reduction of emissions from industry and traffic emissions (e.g. Castellanos and Boersma, 2012; Vrekoussis et al., 2013; Gratsea et al., 2017) and the increase in biomass burning for heating reasons in Southern Europe (e.g. Fameli and Assimakopoulos, 2016). Among other countries across Europe, Greece has been experiencing a number of negative consequences of a severe economic recession since 2010, such as decreased personal income, unprecedented levels of unemployment, more evident in urban regions, as well as large increases in taxation. In particular, the fact that diesel and oil were over-taxed and became too expensive since 2009, led to severe smog episodes by the sudden turn to wood as primary heating fuel (e.g Saffari et al., 2013; Fourtziou et al., 2017). Apart from the more frequent elevated PM_{10} incidents this is thought to also be represented by increased HCHO emissions. Thus, by using HCHO as an air quality tracer, we explore how the HCHO and NO_2 concentrations were affected during the tense period of economic crisis in Greece.

There are very few studies that have used HCHO simulations from air quality models as air quality indicators. Liu, Andreani-Aksoyogly, et al. (2007) used the NILU RCTM chemical transport model to simulate HCHO concentrations in the Po basin (Italy) and, after comparison with ground-based and aircraft measurements performed in the vicinity of Milan in the summer of 2002, assessed that the model can represent well the HCHO levels as well as their temporal and spatial variability. Liu, Flatøy, et al. (2007) used the Comprehensive Air Quality Model with extensions (CAMx) to estimate that > 80% of the HCHO concentrations over the Milan metropolitan region could be photochemically produced from other VOCs. Simulations performed with the use of CAMx revealed that ambient HCHO concentrations in the urban atmosphere of the Mexico City Metropolitan Area are significantly affected by primary HCHO emissions (Lei et al., 2009). Luecken et al. (2012) simulated HCHO over part of the United States using the Community Multiscale Air Quality (CMAQ) model to identify its chemical precursors.

In contrast to in situ measurements which are scarce, satellite HCHO measurements have been collected for nearly three decades using nadir solar backscatter instruments (e.g. Chance et al., 2000). Indicatively, HCHO tropospheric columns have been used from the polar morning orbit GOME-2/MetOp-A and GOME-2/MetOp-B sensors in De Smedt et al. (2012, 2015) and Wang et al. (2017). In Zhu et al. (2016), HCHO columnar data, simulated with the GEOS-Chem chemical transport model over the southeast United States, were used for intercomparison purposes with HCHO columns retrieved from different satellite instruments. Validation of satellite HCHO measurements is also very difficult because ground-based HCHO measurements are extremely sparse. Nevertheless, some validation studies have been reported between satellite HCHO observations and Multi-AXis Differential Optical Absorption Spectroscopy (MAX-DOAS) measurements (e.g. Wittrock et al., 2006; Vigouroux et al., 2009; Wang et al., 2017).

For this work we used HCHO satellite observations to identify possible anthropogenic sources of HCHO emissions over the Greek urban atmosphere during the wintertime since the beginning of the economic crisis in the country. The urban sites selected for this study are Thessaloniki (longitude: 22.971°N, latitude: 40.622°E) and Athens (longitude: 23.773°N, latitude: 37.989°E), two large highly urbanized and densely populated cities with negligible biogenic emissions in winter (Dimitropoulou et al., 2018). Ground-based data sets are also used to check and compare the levels of HCHO vertical column retrievals, while other species relevant to biomass burning, such as nitrogen dioxide (NO_2) were investigated over both cities in order to better understand the origin of the observed HCHO enhancements. According to Wolfe et al. (2016) high NOx concentration levels are often accompanied by increased concentrations of anthropogenic VOC. Finally, we analyzed the satellite HCHO observations against CAMx model simulations to explore if elevated values are captured by the model and to stress the usefulness of satellite measurements in providing representative spatial and temporal distributions of HCHO emissions.

2. Material and methods

2.1. Satellite data sets

The GOME-2 (second Global Ozone Monitoring Experiment) instrument is a nadir viewing UV-VIS spectrometer that measures backscattered solar light (Hassinen et al., 2016). The instrument is mounted on the EUMETSAT (European Organisation for the Exploitation of Meteorological Satellites) MetOp-A (Meteorological Operational satellite-A) and MetOp-B (Meteorological Operational satellite-B) satellites (hereafter GOME-2A and GOME-2B), launched in October 2006 and September 2012, respectively. The main description of the satellites is presented in Table 1 and more details about the GOME-2 instrument are given in Munro et al. (2016) and references therein.

In this study we used the GOME-2 Data Processor Version 4.8 (GDP 4.8), the operational algorithm for the retrieval of total columns of trace gases from the GOME-2 instruments on MetOp-A and MetOp-B, generated at the German Aerospace Center (DLR), as part of the AC-SAF EUMETSAT satellite application facility

on atmospheric composition monitoring. GDP 4.8 is based on Differential Optical Absorption Spectroscopy (DOAS) – based algorithms, originally developed for GOME/ERS-2 (e.g. Spurr et al., 2004). In GDP 4.8, the wavelength regions 328.5–346.0 nm and 425.0–450.0 nm are used for the HCHO and NO_2 retrievals, respectively and cloud parameters are computed directly by the OCRA/ROCINN algorithms (Loyola, 2004; Loyola et al., 2007; Lutz et al., 2016). To reduce the interference between HCHO and BrO absorption features, a two-step DOAS fit retrieval based on De Smedt et al. (2012) that effectively reduces the noise in the GOME-2 HCHO columns has been implemented in the GDP 4.8. The main characteristics of the algorithm

Table 1
Details of satellite instruments.

Instrument	Satellite platform	Global coverage	Equator crossing time (LT)	Pixel size at nadir (km^2)	Study period
GOME-2A	MetOp-A	1.5 day (3 days since July 2013)	09:30	40 × 80 (40 × 40 since July 2013)	2008–2015
GOME-2B	MetOp-B	1.5 day	09:30	40 × 80	2013–2015

Table 2
Main features of satellite algorithm.

	GOME-2A/B HCHO and and NO_2 *GDP4.8*
AMF	Regional Transport Model (RTM) LIDORT v3.7 (Spurr, 2008)
A priori profiles	Chemical Transport Model (CTM) IMAGESv2 (for HCHO) (Stavrakou et al., 2013) and MOZART version 2 (for NO_2) (Horowitz et al., 2003)
Clouds	OCRA (cloud fraction algorithm) and ROCINN (cloud top height and albedo algorithm) (Loyola et al., 2007; Lutz et al., 2016)
Albedo	TOMS/GOME climatology (for HCHO and NO_2) (Boersma et al., 2004)
Aerosol effect	No explicit correction. Corrected indirectly through the OCRA/ROCINN algorithm (Valks et al., 2016)
Monthly averaged column errors	HCHO: 30–80% (De Smedt et al., 2012) and NO_2: 40–80% (Valks et al., 2011)

are presented in Table 2. More details about the GDP4.8 algorithm and the offline products used here are given in the relative algorithm theoretical basis document (Valks et al., 2016) and validation reports, in De Smedt et al. (2015) for the HCHO and in Valks et al. (2011) for the NO_2.

Here we should mention that instruments measuring in the UV and the short-wave visible regions are known to be sensitive to effects of contamination and to degradation of their optical elements. Both GOME-2A and GOME-2B were subject to instrumental degradation since the beginning of their operation (Hassinen et al., 2016 and references therein). Thereby in the GDP4.8 algorithm an equatorial offset correction is applied on a daily basis to the BrO data (Richter et al., 2002) and an empirical degradation correction in the OCRA cloud fraction algorithm softens the instrumental degradation effects and improves the detections (Valks et al., 2016). Moreover, because of the rather small atmospheric absorption of HCHO, the DOAS fit errors often dominate the total uncertainty of the HCHO satellite data (De Smedt et al., 2015). Hence GOME-2 retrievals used in this study are filtered out so as to meet the well-defined data quality criteria that are described in Section 2.4 below.

NO_2 concentrations are strongly located over urban and industrial regions. Since the two species, HCHO and NO_2, have some common main sources in urban areas like the road transport and biomass burning and, in some cases, may exhibit similar emissions and air quality patterns, a comparison between their time series sounds quite sensible and expedient. Details about the filtering of the data intending to single out the quality assured measurements are given in Section 2.4 below. Table 1 performs details of the satellite instrument and data time periods used in this study and Table 2 gives some of the main algorithm' characteristics for the HCHO and NO_2 satellite retrievals.

2.2. Ground-based measurements

Ground-based measurements are essential and increasingly required to quantitatively assess the seasonal variations of the tropospheric HCHO columns. Here, we used independent daily ground-based spectral measurements from a ground-based multi-azimuth MAX-DOAS system located in Penteli (38°.05N, 23°.86E, 527 m a.s.l) within the Athens agglomeration, as well as a MAX-DOAS system located in Thessaloniki (40°.62N, 22°.97E, 60 m a.s.l). The first is a part of the BREDOM network (Bremian DOAS network for atmospheric measurements, http://www.iup.uni-bremen.de/doas/groundbased_data.htm) and is operated at the premises of the National Observatory of Athens. The acquired spectra are analyzed using the DOAS technique (Differential Optical Absorption Spectroscopy, Platt and Stutz, 2008), which applies the Beer-Lambert law. The azimuth angle was set to 52.5° (south direction) pointing at the city centre in order to characterise the urban air quality in Athens. The measurements were performed at +1° elevation angle considering the high altitude above the sea level where the system operates. The fitting windows used for HCHO and NO_2 measurements are 336–359 nm and 425–490 nm, respectively. More information about the instrumentation and data retrieval can be found in Gratsea et al. (2016). The available MAX-DOAS measurements used in this study cover an almost 3.5-year period (October 2012–August 2016). The second dataset of ground-based measurements is provided by a miniature MAX-DOAS system, Phaethon, developed at the Laboratory of Atmospheric Physics, in Thessaloniki (Kouremeti et al., 2013; Drosoglou et al., 2017). The Phaethon system operates on the roof of the Physics Department of the Aristotle University campus in the centre of Thessaloniki. A fixed azimuth angle of 255° was selected as a direction free of significant obstacles for the measurements. The measurements were performed at +30° elevation angle in order to avoid uncertainties introduced due to aerosols at lower elevation angles (Hönninger et al., 2004). The fitting windows used for HCHO and NO_2 measurements are 323–359 nm and 411–445 nm, respectively. The HCHO and NO_2 MAX-DOAS measurements span from November 2013 – June 2016 and May 2011 – December 2015, respectively (Drosoglou et al., 2017).

2.3. Model simulations

The model simulations were derived from the three-dimensional Comprehensive Air Quality Model with extensions (CAMx) (ENVIRON, 2010), using the meteorological fields from the Weather Research and Forecasting model (WRF) (Skamarock et al., 2008). Concentration data and the origin of the boundary conditions are obtained from IFSMOZART model (Morcrette et al., 2009) and the EMEP MSC-W model (Simpson et al., 2012). CAMx simulated HCHO concentrations over a Lambert Conic Conformal grid covering Europe with 141 × 134 grid cells on a 30 km spatial resolution. The domain consisted of 17 vertical layers extending up to about 10 km above ground level, having finer vertical resolution near the ground and coarser in the upper troposphere (the first model layer vertical depth was about 25 m while the depth of the upper layers was on average about 1500 m). CAMx was applied for the year 2009 on a daily basis with an hourly temporal resolution. The gas-phase chemical mechanism used for running CAMx was the 2005 version of Carbon Bond (CB05) including HCHO as an explicit chemical species (Yarwood et al., 2005).

HCHO emissions from anthropogenic sources are obtained from the 2009 annual TNO-MACCII emission database (Kuenen et al., 2014) accounting for the emission sources of energy, industry, residential combustion, transport and waste. More specifically, the annual TNO-MACCII anthropogenic NMVOCs emissions were speciated in 23 chemical species (including HCHO as an explicit chemical species) using source-specific split factors provided by the Netherlands Organisation for Applied Scientific Research (TNO). The split factors for HCHO were the following: 2.9% for energy, 2.4% for residential combustion, 10.2% for industry, 1.7% for road transport, 7.8% for non-road transport and 1.4% for waste. The profiles used for the temporal analysis on an hourly basis of the annual anthropogenic HCHO emissions were based on the GENEMIS temporal profiles (Friedrich, 1997).

Biogenic HCHO emissions were calculated over the CAMx grid on an hourly basis using the Natural Emissions Model (NEMO) driven by the meteorology of WRF (Liora et al., 2015). NEMO calculates isoprene, monoterpenes and other VOCs emissions from vegetation.

More details for the model and emission features and application can be found in Liora et al. (2015)

2.4. Data analysis criteria

Since most of the emitted HCHO originates in the troposphere we suppose that the total HCHO Vertical Column Densities (VCDs) can be used in our study, as has been similarly justified in previous studies (De Smedt et al., 2010; Mahajan et al., 2015). The satellite HCHO and NO_2 data quality filtering was selected according to Valks et al. (2016) and Boersma et al. (2004). Specifically, observation scenes are excluded when cloud fractions are larger than 0.4 for HCHO and 0.2 for NO_2 (cloud radiance fraction > 50%) A solar zenith angle cutoff of 70° is also considered here. The cloud filtering removes a large part of the high aerosol loads, the impact of which is modest in winter compared to summertime retrievals (Boersma et al., 2011; Chimot et al., 2016). Furthermore, all satellite HCHO and NO_2 pixels with their centre coordinates lying within a radius of 50 km from each of the ground-based stations were used in the analysis below and then these observations were averaged within the above distance around each location based on the pixel centre. That was found to be the optimal distance selection in order to obtain a spatially comparable data set and an adequate amount of reliable measurements. Although this screening scheme results in a loss of temporal coverage, which is inevitable in order to mitigate the noise on HCHO observations, the resulting dataset remains appropriate for our analysis.

It should be noted here that the number of observations in winter is lower than in summer and the errors are larger in wintertime. For the winter months, like January, the number of days with good quality satellite observations (pixels) range from 10 to 14 (mostly due to the cloud effect) and the corresponding number of pixels range from 12 to 28 before the daily averaging. The systematic errors that dominate the monthly averages are mostly related to imperfect cloud and aerosols corrections as well as uncertainties in the a priori vertical profile shapes and range between 30–80% for HCHO (De Smedt et al., 2012) and 40–80% for NO_2 (Valks et al., 2011), depending on the number of observations and the season.

The MAX-DOAS observations are formed as the averaged values for all available measurements within 3 h around the satellite overpass time (09:30LT for GOME-2A and B). In terms of the MAX-DOAS measurements the cloud effect found to be negligible according to Gratsea et al. (2016) and Drosoglou et al. (2017), since the most clouds are above the main light path of the viewing direction at the fixed elevation angles of the measurements.

The CAMx HCHO vertical column densities (VCDs) were extracted according to Zyrichidou et al. (2016). The model output was sampled at same time and locations as the GOME-2A overpass.

Finally, we investigated the consistency between the HCHO seasonal variability and the surface temperature using monthly mean temperature station data provided by NASA Goddard Institute for Space Studies (GISS). The data are freely available and accessible to the public at http://data.giss.nasa.gov/gistemp/station_data/ (GISTEMP Team, 2016). More details about the surface temperature data are given in Hansen et al. (2010).

3. Results and discussion

3.1. Satellite data trend analysis

In the upper two plots of Fig. 1 monthly averages of GOME-2A (purple line) and GOME-2B (green line) HCHO total columns (in 10^{15} molecules/cm^2) over Thessaloniki (left panel) and Athens (right panel) from January 2008 to December 2015 are depicted. Overall, GOME2A overestimates the HCHO values, attributed to the more intense GOME-2A instrument degradation and reduced sampling (De Smedt et al., 2015). On a seasonal basis, an increase of HCHO levels in summer and a decline in winter is observed. In summer the GOME-2A observations are in better agreement with the GOME-2B than in winter for their common time period. However, some winter HCHO enhancements (like in year 2011) are detected especially by GOME-2A that should be further investigated below.

In the lower plots of Fig. 1 the temporal variability and evolution of tropospheric NO_2 is shown, which can provide indications for improved understanding as well as attributing the source of the enhanced HCHO observations over the two urban sites in wintertime. In particular, it is observed that the tropospheric NO_2 columns over Thessaloniki are higher or equal to those over Athens during the wintertime of the years 2010 onwards as reported by GOME-2A and GOME-2B retrievals. The two satellite sensors seem to be in better agreement in the case of tropospheric NO_2 columns than for the HCHO ones. In Thessaloniki a slight increase of tropospheric NO_2 is observed by GOME2A from 2010 till 2013 which then gradually declines to lower levels.

Since the GOME-2B dataset period is too short for trend analysis, only GOME-2A is used for studying the annual change of HCHO and NO_2 over both urban sites. We should also mention here that the deseasonalized mean monthly HCHO and NO_2 values (not shown here) depict the same annual patterns and variations and strengthen the results and conclusions of this work. A statistical linear regression analysis that was applied to the deseasonalized time series dataset over Thessaloniki for GOME-2A resulted in a slope of 3.92 ± 0.44% and −3.53 ± 0.05% per annum for HCHO and tropospheric NO_2, respectively. The corresponding slopes over Athens were 4.30 ± 1.32% and −4.60 ± 0.04% for GOME-2A. Worthy of note is that the annual change is positive for HCHO and negative for NO_2 over the study period.

However, in order to determine the dominant reason for the positive HCHO annual change, we included a seasonal term in the trend analysis considering by this way the seasonal variation of HCHO and NO_2. In that respect we selected the cold months November, December, January, February and March and the warm months May, June, July, August and September (according to model seasonal variation of HCHO emissions, see Fig. 2) and seasonal changes per annum were estimated for both HCHO and tropospheric NO_2. For the HCHO observations, the wintertime change per annum was found to be 7.43 ± 2.26% and 6.13 ± 2.12% over Thessaloniki and Athens, respectively, while the summertime trends are found to be lower (2.20 ± 1.88% and 2.59 ± 2.04%). Consequently, it is shown that there is a profound positive winter (and more intense than in summer) HCHO change. Given the fact that the biogenic emissions in winter over both cities are negligible (Dimitropoulou et al., 2018), this increase is likely related to a possible increase of biomass burning emissions in the area given the documented reduction of the road traffic following the dramatic increase in gasoline prices in the country (https://tradingeconomics.com). Previous studies using ground-based and in situ observations have already indicated increased contribution of biomass burning in the winter PM concentrations (Vouitsis et al., 2015; Paraskevopoulou et al., 2015; Florou et al., 2017) and increase in the concentration of wood smoke tracers (e.g. black carbon, potassium, levoglucosan, mannosan, galactosan) (Saffari et al., 2013; Fourtziou et al., 2017) in both cities. In Saffari et al. (2013) the results indicated 30% increase in the $PM_{2.5}$ mass concentration as well as a two and a half fold increase in the concentration of wood smoke tracers in Thessaloniki during the winters of 2012 and 2013.

On the contrary the tropospheric NO_2 winter change per annum was found to be −3.0 ± 0.13% and −3.94 ± 0.14% over Thessaloniki and Athens, respectively, while the corresponding summertime one was −1.58 ± 0.08% and −2.29 ± 0.11%. The aforementioned annual negative tropospheric NO_2 trends are in line with the recent studies of Vouitsis et al. (2015), Sarigiannis et al. (2014) for Thessaloniki (reporting for years 2012–2014) and of Vrekoussis et al. (2013) for Athens (reporting for years 2008–2012). In their work, they show that the marked reduction in traffic activity due to economic factors in the two Greek cities and the subsequent drop in oil consumption appears to be a reasonable cause for the observed reduction in road transport emissions, which constitutes the main source of anthropogenic NO_2 in the

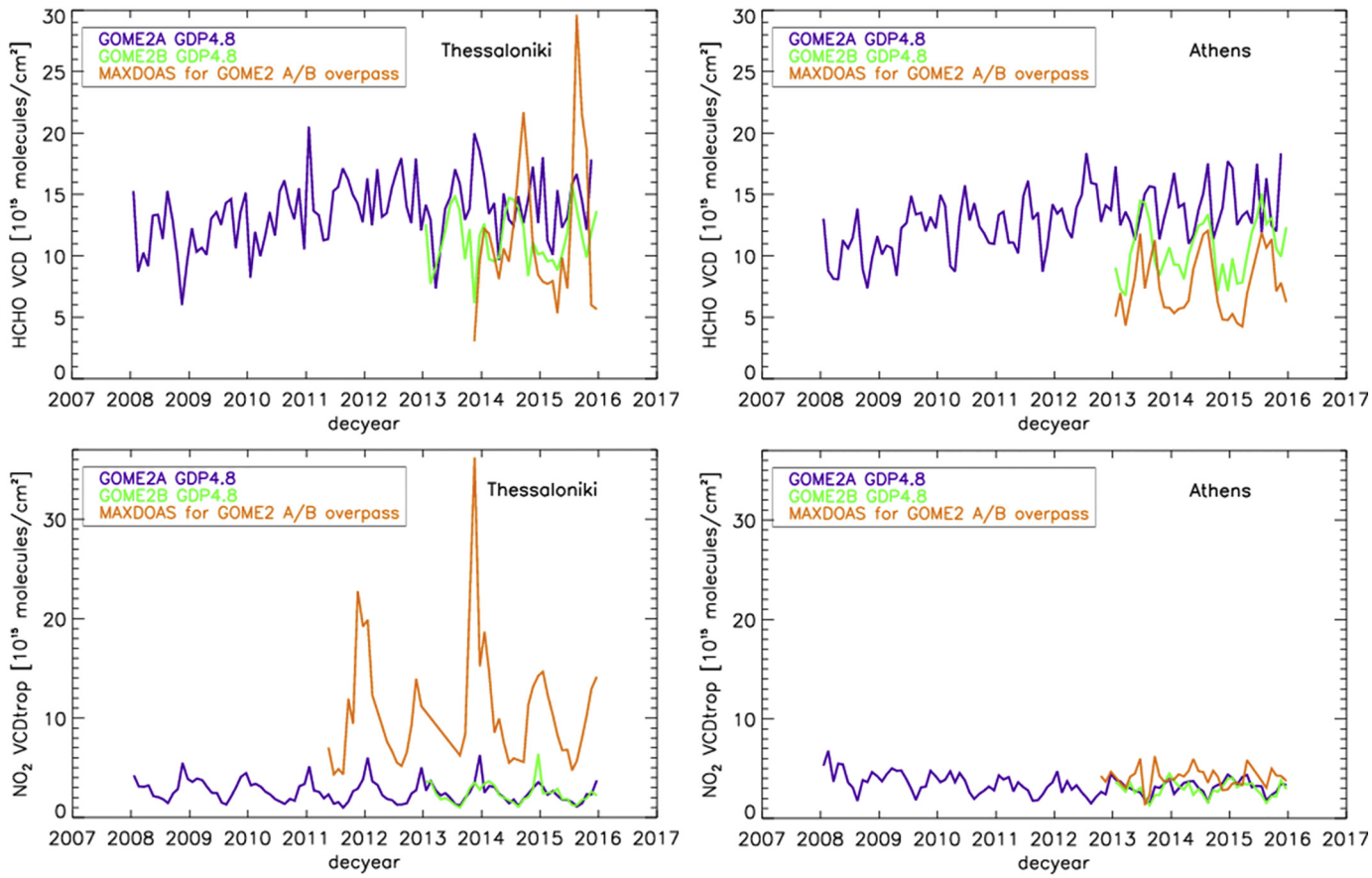

Fig. 1. Monthly mean time series of HCHO total (upper plots) and NO_2 tropospheric (lower plots) VCDs (unit 10^{15} molecules/cm^2) over Thessaloniki (left) and Athens (right) as observed by GOME-2A (purple line) and GOME-2B (green line) sensors and MAX-DOAS instruments around the GOME-2A/B (orange line) overpass time. Note that the "decyear" denotes the decimal year, as well as the different y-axis scale for HCHO and NO_2 plots. (For interpretation of the references to colour in this figure legend, the reader is referred to the web version of this article.)

troposphere. However, in Sarigiannis et al. (2014) it was also reported that between the years 2011 and 2012 a crucial change in emission patterns in Thessaloniki was observed: the traffic component decreased by 30% in 2012, while in the wintertime the component connected with biomass combustion (the ratio of wood smoke $PM_{2.5}/PM_{10}$) excessively went up (from 0.55 up to 0.78 between the warm-cold period). A research that was carried out for Northern Greece and is reported in Slini et al. (2015) was based in a field survey and the results demonstrated that while the consumption of oil and natural gas has been strongly decreased, the retail sales of wood and pellets showed an increase of approximately 600% since the onset of the financial crisis. An increase in the consumption of wood for residential heating of the order of 28% in the time period 2006–2012 in Greece was also reported in Fameli and Assimakopoulos (2016) mainly in large cities. The aforementioned

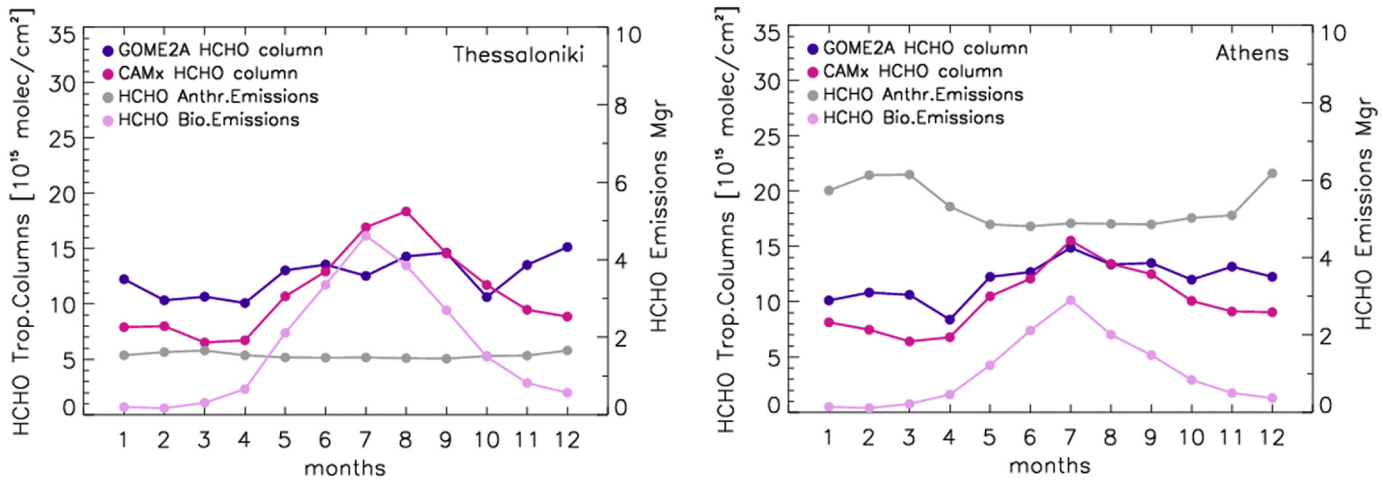

Fig. 2. Annual cycle of HCHO columns as observed by GOME-2A (purple line) and simulated by CAMx (dark pink line) in 10^{15} molecules/cm^2 (left y-axis) and the anthropogenic (grey line) and biogenic (light pink line) HCHO emissions in Mgr (right y-axis) over Thessaloniki (left) and Athens (right). (For interpretation of the references to colour in this figure legend, the reader is referred to the web version of this article.)

studies are entirely in line with the satellite trend analysis found in our study and presented below.

3.2. Comparisons to ground-based observations

The satellite retrieved HCHO and NO_2 are compared to available MAX-DOAS observations (Fig. 1). MAX-DOAS mean monthly HCHO (upper panel) and tropospheric NO_2 (lower panel) measurements, in orange, referred to the GOME-2 overpass time, are depicted over Thessaloniki (left column) and Athens (right column). Ground-based HCHO observations showed a marked peak in summer. The bias between satellite and MAX-DOAS observations can be partly attributed to the different ground pixel sizes and the different a priori profile shapes (Drosoglou et al., 2017), as well as to the fact that the MAX-DOAS instruments have lower sensitivity in the higher altitudes, above about 1–2 km (Wang et al., 2017). MAX-DOAS differences between the two cities are maybe due to different biogenic emissions, mostly in summer (Zyrichidou et al., 2017). However, the important message here is that the satellite HCHO enhancements are captured by the MAX-DOAS HCHO measurements even though the absolute levels do not agree. The mean bias between measurements and observations for the case of HCHO is -2.73×10^{15} molecules/cm^2 over Thessaloniki and -6.42×10^{15} molecules/cm^2 over Athens. In particular, the 2014–2015 winter enhancements are fairly well detected by MAX-DOAS measurements over Thessaloniki, while over Athens it seems that the ground-based instrument slightly underestimates the HCHO load. This fact may be partly attributed to the rather high altitude where the instrument in Athens is located (527 m a.s.l.), which may not sense a significant amount of the surface HCHO. In the lower panels of Fig. 1 the tropospheric NO_2 VCDs retrieved from the MAX-DOAS measurements show the expected annual evolution, with low NO_2 in warm summer conditions compared to the colder months. This seasonality is mainly linked to the chemistry of the hydroxyl radical (OH) and the photolysis frequency of NO_2 (Ordóñez et al., 2016). The mean bias between measurements and observations for the case of NO_2 is 7.93×10^{15} molecules/cm^2 over Thessaloniki (in good relative agreement with the findings in Drosoglou et al., 2017) and 0.92×10^{15} molecules/cm^2 over Athens. A big part of the differences over both cities between satellite and MAX-DOAS NO_2 observations is generally attributed to the different geometries associated with the measured methods of the two instruments. Ground-based measurements are representative of the absorption of radiation in a particular viewing direction and path, while measurements of satellite sensors are sensitive to absorption of radiances emerging from a wide area determined by the size of the satellite pixel. In Drosoglou et al. (2017), in order to overcome this problem and improve the comparisons in the greater area of Thessaloniki, OMI data were adjusted using factors derived from air quality CTM simulations. It was demonstrated that the average difference was reduced (from 6.6 ± 5.71 to $1.68 \pm 5.01 \times 10^{15}$ molecules/cm^2) as far as the tropospheric NO_2 columns were concerned. Another explanation for the differences is the fact that a part of the troposphere is not monitored by MAX-DOAS due to the altitude of the instrument's location coupled with the suburban location of the instrument. This fact may cause an underestimation of the VCDs retrieved from MAX-DOAS. The strength of this effect depends on the vertical distribution of the species, the atmospheric visibility and the observation geometry of the MAX-DOAS measurement. It hence follows that the differences between MAX-DOAS and satellite instrument need to be further investigated in a future analysis, already discussed in Wang et al., 2017.

3.3. Investigating the anthropogenic HCHO component using a CTM model

Since the positive change in HCHO levels (especially in Thessaloniki) during the winter months are mainly connected with enhanced anthropogenic activities, we use a chemical transport model for comparison, validation and further investigation of the seasonality of the HCHO concentrations and emissions. In particular, we exploited a CAMx model run for year 2009, providing consistency between the reference year of the anthropogenic emissions and meteorological data sets used in the model. Fig. 2 illustrates the annual cycle of the HCHO columns as observed by GOME-2A (purple line) and simulated by CAMx (deep pink line) in 10^{15} molecules/cm^2, and the anthropogenic (grey line) and biogenic (light pink line) HCHO emissions in Mgr (right y-axis) over Thessaloniki (left) and Athens (right) for year 2009. It should be noted that as far as the diurnal variation in CAMx emissions (total anthropogenic and residential combustion) is concerned, for all seasons, there is a morning maximum firstly between 6:00–8:00 UTC and a later one between 15:00–17:00 UTC over both cities (not shown here). The morning maximum in winter is higher than the one in summer. The accumulation of direct night-time HCHO emissions could provide large HCHO concentrations at dawn which may lead to morning enhancements, especially in winter. In the winter mornings, the loss of HCHO from the atmosphere is minimized because OH levels are supressed by high NOx concentrations, due to the morning traffic peak, and photolysis is still slow (Parrish et al., 2012).

As seen in Fig. 2, the CAMx simulations show a clear seasonal pattern similar to the seasonality of the biogenic emissions peaking in summer, which is qualitatively in phase with the main crop growing season (April to September) and the surface temperature over both cities. However, in summer, probably the overestimation of the HCHO precursors in photochemical reactions in CAMx or/and the model production mechanism of HCHO lead to higher HCHO concentrations compared to the respective observed values especially over Thessaloniki or on the other hand, the observed ones are underestimated due to the satellite error extend. Finally, the levels of the GOME-2A HCHO columns in the cold months ($\sim 15.0 \times 10^{15}$ molecules/cm^2) are comparable and, in some cases, greater than those during the hot ones, which might further point to the emergence of winter anthropogenic HCHO primary emissions.

These winter enhancements are not captured well by the CAMx anthropogenic emission inventory especially over Thessaloniki.

3.4. The effect of temperature and wood burning on the observed HCHO levels

Fig. 3 illustrates the scatter plots between the long-term mean dataset of mean monthly GOME-2A HCHO VCDs versus the corresponding surface temperature. In the left plots the anti-correlation is well captured over both urban sites with the correlation coefficient, R, found to be negative over both urban cities, -0.3 for Thessaloniki and -0.2 for Athens (left column). There are some winter months, like in 2011 and 2015 (purple and pink dots, respectively) over Thessaloniki and in 2012 and 2013 and 2015 (light brown, dark brown and pink dots, respectively) in Athens, that the GOME-2A HCHO values are unexpectedly and strongly anti-correlated with the surface mean temperature. The stronger anti-correlation over Thessaloniki and such high morning HCHO values ($> 15.0 \times 10^{15}$ molecules/cm^2) in winter both suggest the existence of enhanced antropogenic HCHO emissions. The years of the appearance of this anti–correlation coincide with the beginning of the financial crisis in Greece, in late 2009. As opposed to wintertime, during summer, when the biogenic emissions dominate, the HCHO columns show to be positively correlated with the temperature, with R values 0.5 for Thessaloniki and 0.1 for Athens.

According to climatological statistical data (www.hnms.gr/emy/en/climatology) the monthly mean temperature for January in Athens is 8.7 °C, whereas in Thessaloniki is 5.2 °C. In winter, Athens is hotter than Thessaloniki and with less humidity. To further investigate whether there is a potential link of urban winter HCHO enhancements with the heating demand, we present in Fig. 4 the mean seasonal variability of GOME-2A HCHO VCDs for the years before (2008–2010) and after (2011–2015) the beginning of the economic crisis in Greece. Moreover, we looked into the HCHO seasonal variability over a background site,

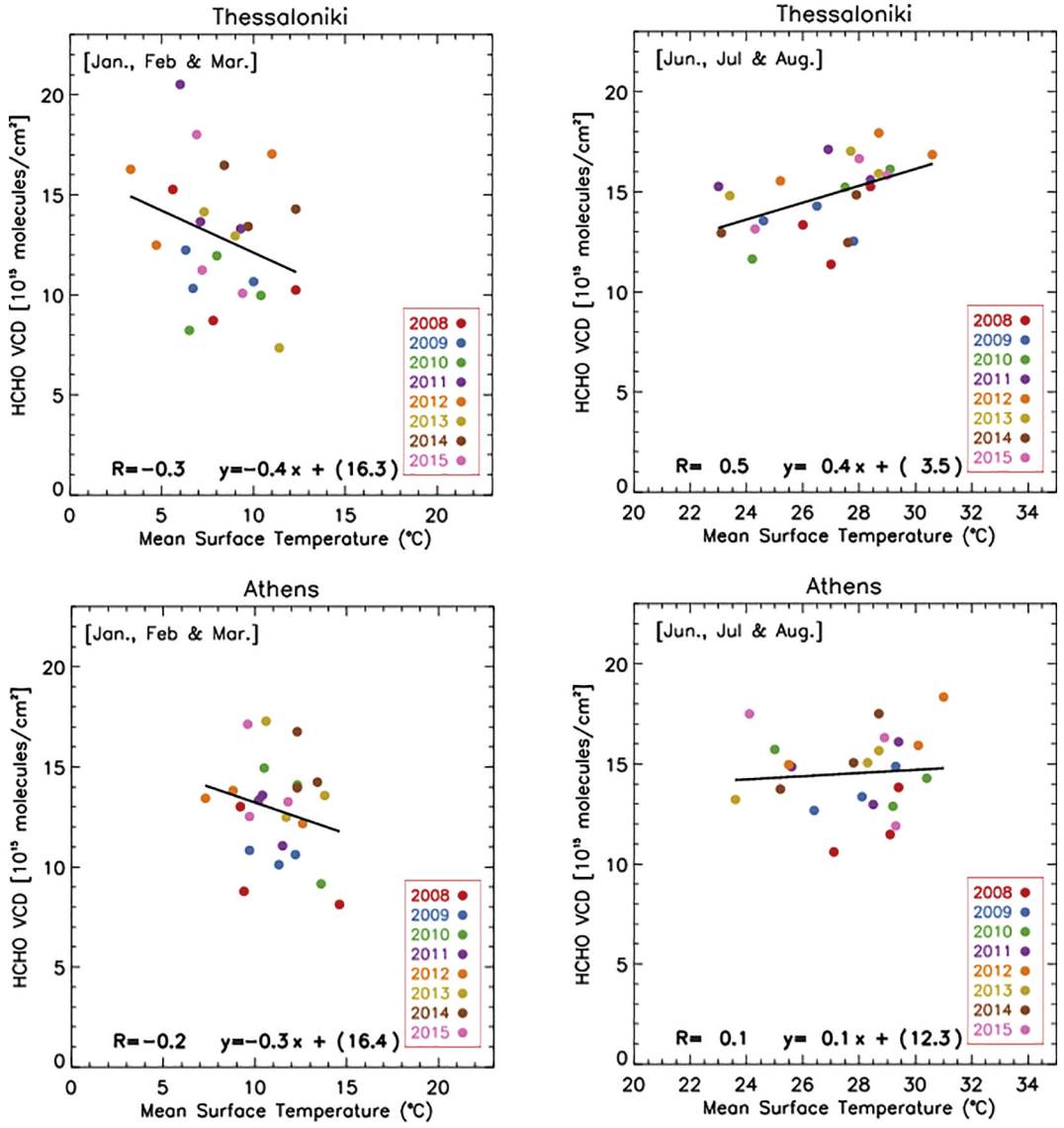

Fig. 3. Scatter plots of GOME-2A HCHO VCDs versus mean surface temperature. Each point represents a winter (left plots) mean monthly value (of the months January, February and March) and a summer (right plots) one (of the months June, July and August) for each geolocation (Thessaloniki: upper plots and Athens: lower plots). The different colours of the dots represent different years. The black solid line represents the linear fit.

Agios Efstratios (25.000°E, 39.516°N), a Greek island in the North Aegean Sea, with no registered anthropogenic activity. We noted, as expected, that there are no significant HCHO fluctuations in the winter values (around 12.0×10^{15} molecules/cm^2 on average) before and after the beginning of the economic crisis over this background site (not shown here). On the contrary, regarding Thessaloniki and Athens from 2011 to 2015, not only the HCHO columns are higher during all seasons compared to the years before (2008–2010), but they are also higher in the cold season than in the warm one over both cities and anti-correlated with the surface temperatures. In the upper right plot of Fig. 4 we illustrate the increase of the retail sales of wood in the greater area of Thessaloniki (by almost 700%) since the beginning of the economic recession [the measurements are courtesy of Slini et al., 2015 and are not available for Athens] and in the lower right plot we demonstrate the energy consumption for residential heating by biomass burning in Greece (in unit PJ). The annual energy consumption (in PJ units) by biomass burning was obtained by the NEDS-MRPEE (National Energy Data System of the Ministry of Reconstruction of Production, Environment and Energy) and the program Odyssee-Mure [Odyssee-Mure project, 2001–2018]. The two red (dark and light) lines in these plots show a remarkable positive trend from 2011 onwards. Given that the monthly average temperatures during the cold season were almost the same for the two time periods, at each site, these findings cannot be attributed to increased necessity for central heating, but rather to anthropogenic HCHO emission activities like the alternative affordable ways of indoor heating (e.g. fireplaces and wood stoves) used during the multi-year recession period. Consequently, the results of Fig. 4 denote a possible relationship between the change in the way Greek people cover their residential heating demand and the wintertime urban HCHO levels in the economically stricken Greece. As shown in Fig. 4, the winters are colder in Thessaloniki than in Athens (about 3.5 °C on average), which means that the heating demand is higher in Thessaloniki and, indeed, equal or higher (like in January) HCHO values have been observed there than in Athens. It is essential to note here that by using another satellite retrieval algorithm for the HCHO columns, namely the Level-2 formaldehyde products of version 14 (developed at BIRA-IASB and openly available on TEMIS [http://h2co.aeronomie.be]), we resulted in almost same anti-correlations (Zyrichidou et al., 2017).

Despite the overall relative connection of our findings with the

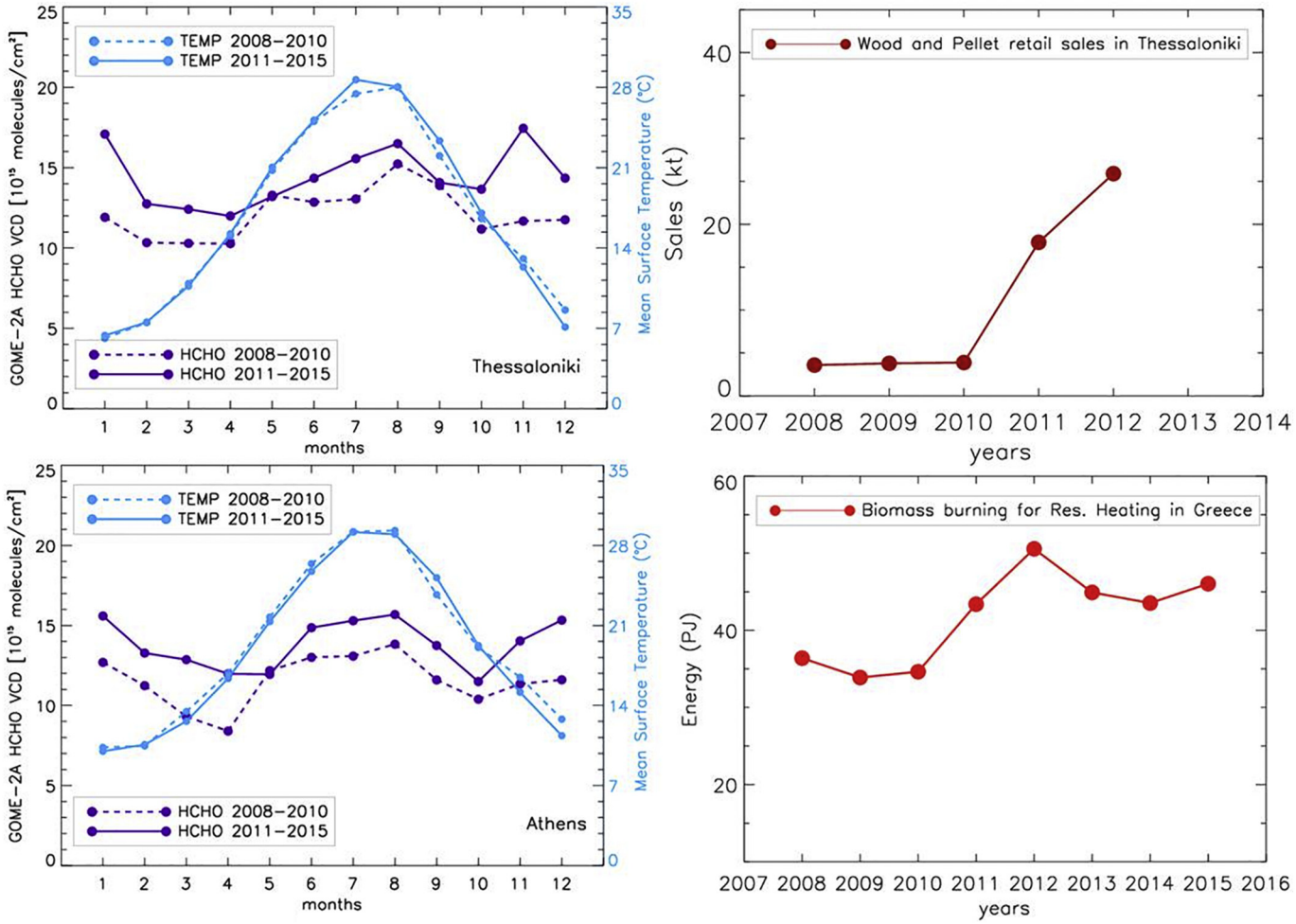

Fig. 4. Left: Mean seasonal variability of GOME-2A HCHO VCDs and averaged surface temperatures for 2008–2010 (dotted purple and light blue lines, respectively) and for 2011–2015 (solid purple and light blue lines, respectively) over Thessaloniki (upper plot) and over Athens (lower plot). **Right:** (upper plot) The wood and pellet retail sales in Thessaloniki (in unit kt) (courtesy of Slini et al., 2015). (lower plot) The energy consumption for residential heating by biomass burning in Greece (in unit PJ) [Odyssee-Mure project, 2014]. (For interpretation of the references to colour in this figure legend, the reader is referred to the web version of this article.)

results of previous studies, concerning the recent gradual reduction in traffic activity, increase in the concentration of wood smoke tracers and increase in biomass burning contribution in the winter PM concentration in Greece, we should mention here that our results cannot be construed as absolutely quantitative, but only indicative. We should be very careful with the absolute interpretation of these findings in numerical levels, due to the large satellite retrievals errors and degradation issues, especially in terms of HCHO, that require further investigation.

4. Conclusions

The financial crisis of 2008 in Europe affected not only the economic sector, but also, among other large European cities, the air quality over Greece. The dire economic condition in Greece which led to the reduced inhabitants' income in combination with the over-taxed energy sector and the increased heating oil prices since 2009 resulted in an exponential increase in the sales and use of woods and pellets for domestic heating in many households creating atmospheric pollution problems during the winter months. Significant HCHO column enhancements were observed from space over urban Greek areas (Thessaloniki, longitude: 22.971°N, latitude: 40.622°E; and Athens, longitude: 23.773°N, latitude: 37.989°E), during wintertime. Following the outbreak of the financial recession in Greece, we explored whether the observed HCHO increases are connected with the intense use of wood for internal heating (fireplaces, wood/pellet stoves) during wintertime. Monthly mean timeseries (2008–2015) of tropospheric HCHO and NO_2 columns over Thessaloniki and Athens derived from the GOME-2A and GOME-2B GDP4.8 observations and their levels were on average good agreement with available MAX-DOAS measurements. However, the absolute differences in HCHO reported levels between satellite and MAX-DOAS observations require further investigation. The deseasonalized timeseries give a positive winter change of 5.30 ± 2.26% and 6.13 ± 2.12% per annum over Thessaloniki and Athens, respectively in the mid-morning for HCHO (from GOME-2A and observations). The statistical linear regression analysis for the summer months resulted in proportional slopes of 2.35 ± 1.88% and 2.59 ± 2.04%. Both winter and summer change per annum of the tropospheric NO_2 is negative, −3.0% and −1.58%, respectively over Thessaloniki, and −3.94% and −2.29% respectively over Athens for GOME-2A, reflecting the reduction in traffic activity due to economic factors in the two Greek cities and the subsequent drop in oil consumption. The GOME-2A HCHO levels since 2010 are higher than those of the previous years, showing a peak in 2011 and 2013 over Thessaloniki and Athens, respectively, while a slight increase is also observed for the GOME-2A tropospheric NO_2. From 2011 to 2015, not only are the GOME-2A HCHO columns higher during all seasons compared to the years before the economic crisis (2008–2010), but they are also higher in the cold season than in the warm one over both cities and anti-correlated with the surface temperatures. The surface temperatures

show an anti-correlation with the HCHO winter over Thessaloniki and Athens (stronger for Thessaloniki with an R of −0.3), that can be an indication of the existence of enhanced anthropogenic HCHO emissions in the urban air. Since the monthly average temperatures during the cold season were almost the same before and after the outbreak of the financial crisis, these findings cannot be attributed to increased necessity for central heating, but rather to increased anthropogenic HCHO emission activities, like the alternative affordable ways of indoor heating (e.g. fireplaces and wood stoves). The confirmed intense use of wood and pellets (in lieu of the expensive heating oil) for heating purposes (e.g. fireplace, pellet stoves) in both cities is consistent with the HCHO and concurrent slight NO_2 winter enhancements and temporally coincide with the onset of the economic recession in Greece.

Such observed winter HCHO enhancements are not captured by the anthropogenic emission inventory used in the CAMx model for year 2009, especially for Thessaloniki. Inverse modelling processes form the next step in this line of work, since the satellite-based emission inventories, i.e. top-down inversions, are capable to scout new emission sources which are absent in the traditional bottom-up inventories. Our study indicates that it is worthwhile, under such socioeconomic and atmospheric pollution circumstances, to use the satellite observations in order to point out the potential of the satellite sensors to assess the air quality and to study the impact of the anthropogenic activity on the urban atmosphere. In the Sentinel era, our long-term motivation is to use high spatiotemporal coverage information of the atmospheric composition of more key air quality species, like SO_2 and CO, that can be provided at an urban scale by satellite atmospheric observations, to improve algorithm retrievals, to get constrained emissions and to update and improve emission inventories in urban atmospheres.

Acknowledgements

Part of this work has been funded in the framework of EUMETSAT's AC SAF project (grant ID: 9100/01.02.2017). We would also like to acknowledge the ESA Sentinel-5 Precursor Level-2 Processor Component Development, PRODEX TRACE-S5P which is currently funding our GOME-2 formaldehyde product developments.

References

Anderson, L.G., Lanning, J.A., Barrell, R., Miyagishima, J., Jones, R.H., Wolfe, P., 1996. Sources and sinks of formaldehyde and acetaldehyde: an analysis of Denver's ambient concentration data. Atmos. Environ. 30, 2113–2123.

Andreae, M.O., Merlet, P., 2001. Emission of trace gases and aerosols from biomass burning. Global Biogeochem. Cy. 15, 955–966.

Boersma, K.F., Eskes, H.J., Brinksma, E.J., 2004. Error analysis for tropospheric NO_2 retrieval from space. J. Geophys. Res. 109, D04311. https://doi.org/10.1029/2003JD003962.

Boersma, K.F., Eskes, H.J., Dirksen, R.J., et al., 2011. An improved tropospheric NO_2 column retrieval algorithm for the ozone monitoring Instrument. Atmos. Meas. Tech. 4, 1905–1928.

Castellanos, P., Boersma, K.F., 2012. Reductions in nitrogen oxides over Europe driven by environmental policy and economic recession. Sci. Rep. 2 (265), 1–7. https://doi.org/10.1038/srep00265.

Chance, K., Palmer, P.I., Spurr, R.J.D., Martin, R.V., Kurosu, T.P., Jacob, D.J., 2000. Satellite observations of formaldehyde over North America from GOME. Geophys. Res. Lett. 27, 3461–3464.

Chimot, J., Vlemmix, T., Veefkind, J.P., de Haan, J.F., Levelt, P.F., 2016. Impact of aerosols on the OMI tropospheric NO2 retrievals over industrialized regions: how accurate is the aerosol correction of cloud-free scenes via a simple cloud model? Atmos. Meas. Tech. 9, 359–382. https://doi.org/10.5194/amt-9-359-2016.

De Smedt, I., Stavrakou, T., Müller, J.F., van Der, A., J, R., Van Roozendael, M., 2010. Trend detection in satellite observations of formaldehyde tropospheric columns. Geophys. Res. Lett. 37, L18808. https://doi.org/10.1029/2010GL044245.

De Smedt, I., et al., 2012. Improved retrieval of global tropospheric formaldehyde columns 15 from GOME-2/MetOp-A addressing noise reduction and instrumental degradation issues. Atmos. Meas. Tech. 5, 2933–2949 (Special Issue: GOME-2: calibration, algorithms, data products and validation).

De Smedt, I., et al., 2015. Diurnal, seasonal and long- term variations of global formaldehyde columns inferred from combined OMI and GOME-2 observations. Atmos. Chem. Phys. 15 (8), 12241–12300. https://doi.org/10.5194/acpd-15-12241-2015.

Dimitropoulou, E., Assimakopoulos, V.D., Fameli, K.M., Flocas, H.A., Kosmopoulos, P., Kazadzis, S., Lagouvardos, K., Bossioli, E., 2018. Estimating the biogenic non-methane hydrocarbon emissions over Greece. Atmosphere 9, 14. https://doi.org/10.3390/atmos9010014. 2018.

Drosoglou, T., Bais, A.F., Zyrichidou, I., Kouremeti, N., Poupkou, A., Liora, N., Giannaros, C., Koukouli, M.E., Balis, D., Melas, D., 2017. Comparisons of ground-based tropospheric NO_2 MAX-DOAS measurements to satellite observations with the aid of an air quality model over Thessaloniki area, Greece. Atmos. Chem. Phys. 17, 5829–5849. https://doi.org/10.5194/acp-17-5829-2017.

ENVIRON, 2010. User's Guide CAMx Comprehensive Air Quality Model with Extensions, Version 5.30. ENVIRON International Corporation.

Fameli, K.M., Assimakopoulos, V.D., 2016. The new open Flexible Emission Inventory for Greece and the Greater Athens Area (FEI-GREGAA): account of pollutant sources and their importance from 2006 to 2012. Atmos. Environ. 137, 17–37.

Favez, O., El Haddad, I., Piot, C., Boreave, A., Abidi, E., Marchand, N., Jaffrezo, J.-L., Besombes, J.-L., Personnaz, M.-B., Sciare, J., Wortham, H., George, C., D'Anna, B., 2010. Inter-comparison of source apportionment models for the estimation of wood burning aerosols during wintertime in an Alpine city (Grenoble, France). Atmos. Chem. Phys. 10, 5295–5314. https://doi.org/10.5194/acp-10-5295-2010.

Florou, K., Papanastasiou, D., Pikridas, M., Kaltsonoudis, C., Louvaris, E., Gkatzelis, E., Patoulias, D., Mihalopoulos, M., Pandis, S., 2017. The contribution of wood burning and other pollution sources to wintertime organic aerosol levels in two Greek cities. Atmos. Chem. Phys. 17, 3145–3163. https://doi.org/10.5194/acp-17-3145-2017.

Fourtziou, L., Liakakou, E., Stavroulas, I., Theodosi, C., Zarmpas, P., Psiloglou, B., Sciare, J., Maggos, T., Bairachtari, K., Bougiatioti, A., Gerasopoulos, E., Sarda-Esteve, R., Bonnaire, N., Mihalopoulos, N., 2017. Multi-tracer approach to characterize domestic wood burning in Athens (Greece) during wintertime. Atmos. Environ. 148, 89–101. https://doi.org/10.1016/j.atmosenv.2016.10.011.

Fried, A.., et al., 2003. Airborne tunable diode laser measurements of formaldehyde during TRACE-P: distributions and box model comparisons. J. Geophys. Res.-Atmos. 108 (D20), 8798. https://doi.org/10.1029/2003JD003451.

Friedrich, R., 1997. GENEMIS: assessment, improvement, temporal and spatial disaggregation of European emission data. In: Ebel, A., Friedrich, R., Rhode, H. (Eds.), Tropospheric Modelling and Emission Estimation, (PART 2). Springer, New York.

GISTEMP Team, 2016. GISS Surface Temperature Analysis (GISTEMP). NASA Goddard Institute for Space Studies.

Gratsea, N., Liakakou, E., Mihalopoulos, N., Adamopoulos, A., Tsilibari, E., Gerasopoulos, E., 2017. The combined effect of reduced fossil fuel consumption and increasing biomass combustion on Athens' air quality, as inferred from long term CO measurements. Sci. Total Environ. 592, 115–123. https://doi.org/10.1016/j.scitotenv.2017.03.045.

Gratsea, M., Vrekoussis, M., Richter, A., Wittrock, F., Schonhardt, A., Burrows, J., Kazadzis, S., Mihalopoulos, N., Gerasopoulos, E., 2016. Slant column MAX-DOAS measurements of nitrogen dioxide, formaldehyde, glyoxal and oxygen dimer in the urban environment of Athens. Atmos. Environ. 135, 118–131. https://doi.org/10.1016/j.atmosenv.2016.03.048.

Hansen, J., Ruedy, R., Sato, M., Lo, K., 2010. Global surface temperature change. Rev. Geophys. 48, RG4004. https://doi.org/10.1029/2010RG000345.

Hassinen, S., et al., 2016. Overview of the O3M SAF GOME-2 operational atmospheric composition and UV radiation data products and data availability. Atmos. Meas. Tech. 9, 383–407.

Hönninger, G., von Friedeburg, C., Platt, U., 2004. Multi axis differential optical absorption spectroscopy. Atmos. Chem. Phys. 4 231e254. (1680-7324/acp/2004-4-231).

Horowitz, L., Walters, S., Mauzerall, D., et al., 2003. A global simulation of tropospheric ozone and related tracers: description and evaluation of MOZART, version 2. J. Geophys. Res. 108, 4784. https://doi.org/10.1029/2002JD002853.

Kouremeti, N., Bais, A.F., Balis, D., Zyrichidou, I., 2013. Phaethon, a system for the validation of satellite derived atmospheric columns of trace gases. In: Helmis, C.G., Nastos, P.T. (Eds.), Advances in Meteorology, Climatology and Atmospheric Physics. Springer, Berlin Heidelberg, pp. 1081–1088. https://doi.org/10.1007/978-3-642-29172-2_151.

Kuenen, J.J.P., et al., 2014. TNO-MACC_II emission inventory; a multi-year (2003–2009) consistent high-resolution European emission inventory for air quality modelling. Atmos. Chem. Phys. 14, 10963–10976. https://doi.org/10.5194/acp-14-10963-2014.

Lathiere, J., et al., 2006. Impact of climate variability and land use changes on global biogenic volatile organic compound emissions. Atmos. Chem. Phys. 6, 2129–2146. https://doi.org/10.5194/acp-6-2129-2006.

Lawson, D.R., Bierman, H.W., Tuazon, E.C., et al., 1990. Formaldehyde measurements methods evaluation and ambient concentrations during the carbonaceous species methods comparison study. Aerosol Sci. Technol. 12, 64–76.

Lee, M., Heikes, B.G., Jacob, D.J., Sachse, G., Anderson, B., 1997. Hydrogen peroxide, organic peroxides, and formaldehyde as primary pollutants from biomass burning. J. Geophys. Res. 102, 1301–1309.

Lei, W., Zavala, M., de Foy, B., Volkamer, R., Molina, M.J., Molina, L.T., 2009. Impact of primary formaldehyde on air pollution in the Mexico City Metropolitan Area. Atmos. Chem. Phys. 9, 2607–2618.

Liora, N., Markakis, K., Poupkou, A., Giannaros, T.M., Melas, D., 2015. Atmos. Environ. 122, 493–504. https://doi.org/10.1016/j.atmosenv.2015.10.014.

Liu, L., Andreani-Aksoyoglu, S., Keller, J., Ordonez, C., Junkermann, W., Hak, C., Braathen, G.O., Reimann, S., Astorga-Llorens, C., Schultz, M., Prevot, A.S.H., Isaksen, I.S.A., 2007. A photochemical modeling study of ozone and formaldehyde generation and budget in the Po basin. J. Geophys. Res. 112, D22303. https://doi.org/10.1029/2006JD008172.

Liu, L., Flatøy, F., Ordonez, C., Braathen, G.O., Hak, C., Junkermann, W., Andreani-Aksoyoglu, S., Mellqvist, J., Galle, B., Prevot, A.S.H., Isaksen, I.S.A., 2007. Photochemical modelling in the Po basin with focus on formaldehyde and ozone. Atmos. Chem. Phys. 7, 121–137.

Lowe, D.C., Schmidt, U., 1983. Formaldehyde (HCHO) measurements in the nonurban atmosphere. J. Geophys. Res. 88, 10844–10858 (1983).
Loyola, D., 2004. Automatic cloud analysis from polar-orbiting satellites using neural network and data fusion techniques. IEEE Intern. Geosci. Rem. Sens. Symp. 4, 2530–2534 Alaska.
Loyola, D., Thomas, W., Livschitz, Y., Ruppert, T., Albert, P., Hollmann, R., 2007. Cloud properties derived from GOME/ERS-2 backscatter data for trace gas retrieval. IEEE Trans. Geosci. Rem. Sens. 45 (9), 2747–2758.
Luecken, D.J., Hutzell, W.T., Strum, M.L., Pouliot, G.A., 2012. Regional sources of atmospheric formaldehyde and acetaldehyde, and implications for atmospheric modelling. Atmos. Environ. 47, 477–490.
Lutz, R., Loyola, D., Gimeno García, S., Romahn, F., 2016. OCRA radiometric cloud fractions for GOME-2 on MetOp-A/B. Atmos. Meas. Tech. 9, 2357–2379. https://doi.org/10.5194/amt-9-2357-2016.
Mahajan, A.S., De Smedt, I., Biswas, M.S., et al., 2015. Inter-annual variations in satellite observations of nitrogen dioxide and formaldehyde over India. Atmos. Environ. 116, 194–201. https://doi.org/10.1016/j.atmosenv.2015.06.004.
Marbach, T., Beirle, S., Platt, U., Hoor, P., Wittrock, F., Richter, A., Vrekoussis, M., Grzegorski, M., Burrows, J.P., Wagner, T., 2009. Satellite measurements of formaldehyde linked to shipping emissions. Atmos. Chem. Phys. 9, 8223–8234. https://doi.org/10.5194/acp-9-8223-2009.
Morcrette, J.-J., et al., 2009. Aerosol analysis and forecast in the European centre for medium-range weather forecasts integrated forecast system: forward modelling. J. Geophys. Res. 114, D06206. https://doi.org/10.1029/2008JD011235.
Munro, R., Lang, R., Klaes, D., et al., 2016. The GOME-2 instrument on the Metop series of satellites: instrument design, calibration, and level 1 data processing – an overview. Atmos. Meas. Tech. 9 (3), 1279–1301. https://doi.org/10.5194/amt-9-1279-2016.
Ordóñez, C., Richter, A., Steinbacher, M., 2016. Comparison of 7 years of satellite-borne and ground-based tropospheric NO_2 measurements around Milan, Italy. J. Geophys. Res. 111https://doi.org/10.1029/2005JD006305. D05310.
Paraskevopoulou, D., Liakakou, E., Gerasopoulos, E., Mihalopoulos, N., 2015. Sources of atmospheric aerosol from long-term measurements (5 years) of chemical composition in Athens, Greece. Sci. Total Environ. 527–528, 165–178. https://doi.org/10.1016/j.scitotenv.2015.04.022.
Parrish, D.D., et al., 2012. Primary and secondary sources of formaldehyde in urban atmospheres: Houston Texas region. Atmos. Chem. Phys. 12, 3273–3288.
Platt, U., Stutz, J., 2008. Differential Optical Absorption Spectroscopy. Springer-Verlag, Berlin Heidelberg (ISBN: 978-3-540-21193-8).
Richter, A., Wittrock, F., Ladstäatter-Weißenmayer, A., Burrows, J.P., 2002. GOME measurements of stratospheric and tropospheric BrO. Adv. Space Res. 29, 1667–1672.
Saffari, A., Daher, N., Samara, C., Voutsa, D., Kouras, A., Manoli, E., Karagkiozidou, O., Vlachokostas, C., Moussiopoulos, N., Shafer, M.M., Schauer, Ja.J., Sioutas, C., 2013. Increased biomass burning due to the economic crisis in Greece and its adverse impact on wintertime air quality in Thessaloniki. Environ. Sci. Technol. 47, 13313–13320. https://doi.org/10.1021/es403847h.
Sander, S.P., et al., 2006. Chemical Kinetics and Photochemical Data for Use in Atmospheric Studies. (Rep. 06-2, 523 pp., Jet Propul. Lab., Pasadena, Calif).
Sarigiannis, D.A., Karakitsios, S.P., Kermenidou, M., et al., 2014. Total exposure to airborne particulate matter in cities: the effect of biomass combustion. Sci. Total Environ. 493, 795–805.
Seco, R., Peñuelas, J., Filella, I., 2007. Short-chain oxygenated VOCs: emission and uptake by plants and atmospheric sources, sinks, and concentrations. Atmos. Environ. 41, 2477–2499. https://doi.org/10.1016/j.atmosenv.11.029.
Shim, C., Wang, Y., Choi, Y., Palmer, P.I., Abbot, D.S., Chance, K., 2005. Constraining global isoprene emissions with global ozone monitoring experiment (GOME) formaldehyde column measurements. J. Geophys. Res. 110, D24301. https://doi.org/10.1029/2004JD005629.
Simpson, D., Benedictow, A., Berge, H., et al., 2012. The EMEP MSC-W chemical transport model–technical description. Atmos. Chem. Phys. 12, 7825–7865. https://doi.org/10.5194/acp-12-7825-2012.
Singh, H.B., et al., 2000. Distribution and fate of selected oxygenated organic species in the lower troposphere and lower stratosphere over the Atlantic. J. Geophys. Res. 105, 3795–3805.
Skamarock, W.C., et al., 2008. A description of the Advanced Research WRF version 3. (NCAR Technical Note, NCAR/TN-475 + STR, June 2008, Boulder Colorado, USA, 125).
Slini, T., Giama, E., Papadopoulos, A.M., 2015. The impact of economic recession on domestic energy consumption. Int. J. Sustain. Energy 34 (3–4), 259e270. https://doi.org/10.1080/14786451.2014.882335.
Spurr, R., 2008. LIDORT and VLIDORT: linearized pseudo-spherical scalar and vector discrete ordinate radiative transfer models for use in remote sensing retrieval problems. In: Kokhanovsky, A. (Ed.), Light Scattering Reviews. vol. 3. Springer, Berlin, pp. 229–275. https://doi.org/10.1007/978-3-540- 48546-97.
Spurr, R.J.D., Van Roozendael, M., Loyola, D.G., 2004. Algorithm Theoretical Basis Document for GOME Total Column Densities of Ozone and Nitrogen Dioxide. P/GDOAS: GDP 4.0. (ERSE-DTEXEOPG-TN-04-0007, Iss./Rev.:1/A).
Stavrakou, T., Müller, J.-F., Boersma, K.F., et al., 2013. Key chemical NOx sink uncertainties and how they influence top-down emissions of nitrogen oxides. Atmos. Chem. Phys. 13, 9057–9082. https://doi.org/10.5194/acp-13-9057-2013.
Stavrakou, T., Muller, J.-F., De Smedt, I., Van Roozendael, M., van der Werf, G.R., Giglio, L., Guenther, A., 2009. Evaluating the performance of pyrogenic and biogenic emission inventories against one decade of space-based formaldehyde columns. Atmos. Chem. Phys. 9, 1037–1060. https://doi.org/10.5194/acp-9-1037-2009.
Valks, P., Pinardi, G., Richter, A., Lambert, J.-C., Hao, N., Loyola, D., Van Roozendael, M., Emmadi, S., 2011. Operational total and tropospheric NO_2 column retrieval for GOME-2. Atmos. Meas. Tech. 4, 1491–1514.
Valks, P., et al., 2016. Product User Manual for GOME Total Column Products of Ozone, NO_2, BrO, HCHO, SO_2, H_2O and Cloud Properties. (GDP 4.8, DLR/GOME/PUM/01, Iss./Rev. 3/A, Oct. 2016).
Vigouroux, C., Hendrick, F., Stavrakou, T., Dils, B., De Smedt, I., Hermans, C., Merlaud, A., Scolas, F., Senten, C., Vanhaelewyn, G., Fally, S., Carleer, M., Metzger, J.-M., Müller, J.-F., Van Roozendael, M., De Mazière, M., 2009. Ground-based FTIR and MAX-DOAS observations of formaldehyde at Réunion Island and comparisons with satellite and model data. Atmos. Chem. Phys. 9, 9523–9544. https://doi.org/10.5194/acp-9-9523-2009.
Vouitsis, I., Amanatidis, S., Ntziachristos, L., Kelessis, A., Petrakakis, M., Stamos, I., Mitsakis, E., Samaras, Z., 2015. Daily and seasonal variation of traffic related aerosol pollution in Thessaloniki, Greece, during the financial crisis. Atmos. Environ. 122 (2015), 577–587.
Vrekoussis, M., Richter, A., Hilboll, A., et al., 2013. Economic crisis detected from space: Air quality observations over Athens/Greece. Geophys. Res. Lett. 40, 458–463. https://doi.org/10.1002/grl.50118.
Wang, Y., Beirle, S., Lampel, J., et al., 2017. Validation of OMI, GOME-2A and GOME-2B tropospheric NO_2, SO_2 and HCHO products using MAX-DOAS observations from 2011 to 2014 in Wuxi, China: investigation of the effects of priori profiles and aerosols on the satellite products. Atmos. Chem. Phys. 17, 5007–5033. https://doi.org/10.5194/acp-17-5007-2017.
Wittrock, F., Richter, A., Oetjen, H., Burrows, J.P., Kanakidou, M., Myriokefalitakis, S., Volkamer, R., Beirle, S., Platt, U., Wagner, T., 2006. Simultaneous global observations of glyoxal and formaldehyde from space. Geophys. Res. Lett. 33https://doi.org/10.1029/2006GL026310. L16804.
Wolfe, G.M., Kaiser, J., Hanisco, T.F., et al., 2016. Formaldehyde production from isoprene oxidation across NOx regimes. Atmos. Chem. Phys. 16, 2597–2610. https://doi.org/10.5194/acp-16-2597-2016.
Yarwood, G., Rao, S., Yocke, M., Whitten, G.Z., 2005. Updates to the carbon bond chemicalmechanism: CB05. Final Report Prepared for US EPA, RT-04-00675. http://www.camx.com/publ/pdfs/CB05_Final_Report_120805.pdf.
Zhu, L., Jacob, D.J., Kim, P.S., Fisher, J.A., Yu, K., Travis, K.R., Mickley, L.J., Yantosca, R.M., Sulprizio, M.P., De Smedt, I., Abad, G.G., Chance, K., Li, C., Ferrare, R., Fried, A., Hair, J.W., Hanisco, T.F., Richter, D., Scarino, A.J., Walega, J., Weibring, P., Wolfe, G.M., 2016. Observing atmospheric formaldehyde (HCHO) from space: validation and intercomparison of six retrievals from four satellites (OMI, GOME2A, GOME2B, OMPS) with SEAC4RS aircraft observations over the southeast US. Atmos. Chem. Phys. 16, 13477–13490.
Zyrichidou, I., Balis, D., Liora, N., et al., 2017. Investigating the impact of the economic recession over Mediterranean urban regions on satellite-based formaldehyde columns; comparison with chemistry transport model results. In: Perspectives on Atmospheric Sciences. Springer International Publishing, Thessaloniki, Greece, pp. 1027–1033. XIII EMTE National-International Conference of Meteorology-Climatology and Atmospheric Physics, September 19–21. online ISBN: 978-3-319-35095-0. https://doi.org/10.1007/978-3-319-35095-0_147.